

Signal Flow Graph in Loop Gain Analysis of DC–DC PWM CCM Switching Converters

Wing-Hung Ki, *Member, IEEE*

Abstract—A systematic and unified method using the signal flow graph (SFG) technique is presented in analyzing dc–dc pulsewidth modulated (PWM) switch mode power converters (SMPC's) operating in the continuous conduction mode (CCM). Loop gains for single and multiloop systems are reviewed. The SFG of the converter is then generated from the perturbed state-space averaged (SSA) equations, and the characteristic polynomial of the system is computed. By grouping terms associated with the gain of the error amplifier as the numerator, a unique definition of system loop gain is introduced, and locations for breaking the loop are discussed. System loop gains for both voltage- and current-programming converters with either trailing- or leading-edge modulation are derived. It is shown that for a SMPC, the loop gain measured by an analog injection method is the system loop gain, which determines the stability of the converter.

Index Terms—Loop gain analysis, signal flow graph analysis, switch mode power converters.

I. INTRODUCTION

STATE-SPACE averaging (SSA) is a useful method in the small signal analysis of dc–dc pulsewidth modulated (PWM) switch mode power converters (SMPC's or switching converters) [1]. It has worked satisfactorily in predicting the performance of continuous conduction mode (CCM) converters employing either voltage programming [1] or current programming [2], [3] with slope compensation [4], [5], in computing input and output impedances [6], [7], and in analyzing converters with leading-edge modulation [8]. A switching flow-graph method was developed to perform SSA [9] graphically and similar results were obtained.

Different analyses have different insufficiencies, which are discussed next. In [1], [2], [5], and [7], the perturbed SSA equation is derived in relating the input vector $\hat{u}(t)$ and the state vector $\hat{x}(t)$ [and its derivative $\dot{\hat{x}}(t)$] with the duty ratio \hat{d} (Table I). After perturbation analysis is performed, the discussions turn to the development of circuit modeling of converters. This so-called hybrid modeling very often generates different models for different converters, e.g., the canonical model for voltage-programming converters [1] is different from that of the current-programming converters [4]. Moreover, these models do not differentiate between trailing-

and leading-edge modulated converters, which were shown to have different dynamics [8]. Second, in [3] systematic application of matrix computation has been adopted and in doing so, loop gains, input, and output impedances are written down in compact matrix notation. In [3], (3) and (4) of this article were used to compute the loop gain of the converter, with the state vector \hat{x} in (4) regarded as the input vector to the loop. This assignment is quite arbitrary and is not compatible with the definition of loop gain if signal flow graph (SFG) analysis [10] is to be used. Moreover, it shows its weakness when a current-programming converter is analyzed, with pole locations different from those obtained in [4]. Third, to evaluate the validity of an analysis, loop gain measurement should be performed. In this aspect, both analog [11] and digital [12] injection methods were suggested. For voltage-programming converters, the loop gains measured by both techniques are compatible, yet those of current-programming converters differ [12]. This discrepancy has to be resolved, but so far, no attempt has been made.

With the above background in mind, a unified method in analyzing SMPC's is needed that: 1) does not require different models for different converters; 2) generates analytical results that are consistent with measurements; and 3) explains the discrepancy between analog and digital loop gain measurements. Such method is established by using SSA coupled with SFG as the vehicles for analysis.

The proposed method is introduced with a review on loop gains in SFG analysis, and the correct procedure in breaking a loop is discussed in Section II. The dynamics of a converter is described by sets of differential equations in different states and SSA is then employed to obtain the averaged equations (Table I). The loop is closed by installing an appropriate controller that is modeled by a control equation that depends on the control method. By perturbing the averaged equations and identifying the perturbed state variables, the corresponding SFG can be constructed, which is the same for both the voltage- and the current-programming converters (Section III). The determinant of the graph is then computed. By using the loop-breaking technique discussed in Section II, and by grouping terms that contain the gain of the error amplifier as the numerator, a unique system loop gain can be defined (Section III). The above method is then applied to analyze the generic buck–boost and boost converters (Section IV), while results of the buck converter are included for completeness. Verification of the analysis is presented in Section V. It is noted that the loops for analog and digital injection are broken at different locations, which explains the discrepancy

Manuscript received September 1, 1996; revised February 8, 1997, July 15, 1997, and December 1, 1997. This work was supported in part by the Hong Kong Research Grant Council under Grant HKUST765/96E. This paper was recommended by Associate Editor L. Martinez-Salamero.

The author is with the Department of Electrical & Electronic Engineering, The Hong Kong University of Science & Technology, Clear Water Bay, Hong Kong (e-mail: eeki@ee.ust.hk).

Publisher Item Identifier S 1057-7122(98)02825-6.

TABLE I
SUMMARY OF ANALYSIS

State vector : $\mathbf{x}(t) = \begin{bmatrix} v_c \\ i_l \end{bmatrix}$	Input vector : $\mathbf{u}(t) = \begin{bmatrix} v_g \\ i_2 \end{bmatrix}$	Output vector : $\mathbf{y}(t) = \begin{bmatrix} v_o \\ i_g \end{bmatrix}$
State 1 : $\dot{\mathbf{x}}(t) = \mathbf{A}_1\mathbf{x} + \mathbf{B}_1\mathbf{u}$ $\mathbf{y}(t) = \mathbf{C}_1\mathbf{x} + \mathbf{D}_1\mathbf{u}$	State 2 : $\dot{\mathbf{x}}(t) = \mathbf{A}_2\mathbf{x} + \mathbf{B}_2\mathbf{u}$ $\mathbf{y}(t) = \mathbf{C}_2\mathbf{x} + \mathbf{D}_2\mathbf{u}$	
Define	$\mathbf{M} = \mathbf{D}\mathbf{M}_1 + \mathbf{D}'\mathbf{M}_2$ gives the averaged model	
	$\dot{\hat{\mathbf{x}}}(t) = \mathbf{A}\hat{\mathbf{x}} + \mathbf{B}\hat{\mathbf{u}}$ $\hat{\mathbf{y}}(t) = \mathbf{C}\hat{\mathbf{x}} + \mathbf{D}\hat{\mathbf{u}}$	
DC Analysis :	$\mathbf{x}_o = \begin{bmatrix} V_c \\ I_l \end{bmatrix} = -\mathbf{A}^{-1}\mathbf{B}\mathbf{u}_o$ where $\mathbf{u}_o = \begin{bmatrix} V_g \\ 0 \end{bmatrix}$ $\mathbf{y}_o = \begin{bmatrix} V_o \\ I_g \end{bmatrix} = [-\mathbf{C}\mathbf{A}^{-1}\mathbf{B} + \mathbf{D}]\mathbf{u}_o$ $\eta = \frac{V_o I_o}{V_g I_g}$	
Perturbation analysis :	\mathbf{v} changes to $\mathbf{v} + \hat{\mathbf{v}}$ \mathbf{D} changes to $\mathbf{D} + \hat{\mathbf{d}}$	
gives	$\dot{\hat{\mathbf{x}}}(t) = \mathbf{A}\hat{\mathbf{x}} + \mathbf{B}\hat{\mathbf{u}} + \mathbf{E}\hat{\mathbf{d}}$ $\hat{\mathbf{y}}(t) = \mathbf{C}\hat{\mathbf{x}} + \mathbf{D}\hat{\mathbf{u}} + \mathbf{F}\hat{\mathbf{d}}$	
where	$\mathbf{E} = (\mathbf{A}_1 - \mathbf{A}_2)\mathbf{x}_o + (\mathbf{B}_1 - \mathbf{B}_2)\mathbf{u}_o$ $\mathbf{F} = (\mathbf{C}_1 - \mathbf{C}_2)\mathbf{x}_o + (\mathbf{D}_1 - \mathbf{D}_2)\mathbf{u}_o$	
Note that :	$\hat{\mathbf{d}} = \hat{\mathbf{d}}(\hat{\mathbf{x}}(t), \hat{\mathbf{u}}, \hat{v}_e(\hat{\mathbf{x}}, \hat{\mathbf{u}}))$ $\Rightarrow \hat{\mathbf{d}} = \mathbf{G}\hat{\mathbf{x}} + \mathbf{H}\hat{\mathbf{u}}$	
Loop Gains Analysis :	$\dot{\hat{\mathbf{x}}}(t) = \mathbf{A}\hat{\mathbf{x}} + \mathbf{E}\mathbf{G}\hat{\mathbf{x}}$ $\Delta = \det[s\mathbf{I} - \mathbf{A} - \mathbf{E}\mathbf{G}]$	
1) Voltage programming :	$\mathbf{G} = \mathbf{A}(s)\mathbf{b}\mathbf{G}_a$ $T(s) = -\text{trace}([s\mathbf{I} - \mathbf{A}]^{-1}\mathbf{E}\mathbf{G})$ $= -\mathbf{A}(s)\mathbf{b} \frac{\text{trace}(\text{adj}(s\mathbf{I} - \mathbf{A})\mathbf{E}\mathbf{G}_a)}{\det(s\mathbf{I} - \mathbf{A})}$	
2) Current programming :	$\mathbf{G} = \mathbf{A}(s)\mathbf{b}\mathbf{G}_a + \mathbf{G}_b$ $T(s) = -\text{trace}([s\mathbf{I} - \mathbf{A} - \mathbf{E}\mathbf{G}_b]^{-1}\mathbf{E}\mathbf{G}_a)$ $= -\mathbf{A}(s)\mathbf{b} \frac{\text{trace}(\text{adj}(s\mathbf{I} - \mathbf{A})\mathbf{E}\mathbf{G}_a)}{\det(s\mathbf{I} - \mathbf{A} - \mathbf{E}\mathbf{G}_b)}$	

in these measurements. The analysis also deals with trailing- and leading-edge modulated converters on the same setting by using the correct control equations governed by the actual switching action.

To facilitate our discussion, a concise summary of SSA analysis is tabulated in Table I. Input, output, and state vectors are represented by boldfaced lower case letters \mathbf{u} , \mathbf{y} , and \mathbf{x} , respectively, while matrices \mathbf{A} , \mathbf{B} , \mathbf{C} , and \mathbf{D} follow the conventional assignment in control theory [13], as in [1] and [3]. The remaining matrices are assigned alphabetically in the order of appearance. Note that row vectors are not written as transposed column vectors. Perturbed quantities are represented by hatted letters, such as $\hat{\mathbf{x}}$ and $\hat{\mathbf{d}}$. Researchers in the field of power electronics should find Table I self-explanatory up to the computation of the system loop gain, which is the major topic of this article.

II. LOOP GAINS OF AN SFG

The SFG of any converter with (perturbed SSA) capacitor voltage and inductor current as state variables has more than one loop. It is well known that loop gains are not uniquely defined [4] and some may not be practical in determining the stability of the converter. To resolve this ambiguity, a review

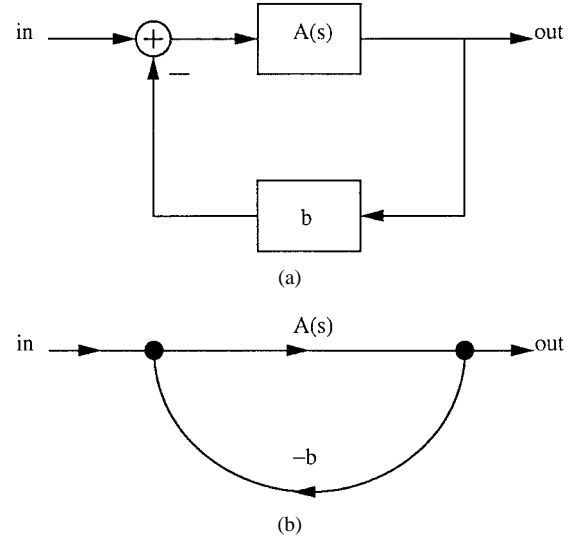


Fig. 1. (a) Block diagram of a single loop system and (b) SFG of a single loop system.

on the definition of loop gains based on the SFG analysis is presented.

A. Loop Gain of a Single Loop System

Fig. 1 shows the block diagram of a single loop system. The forward gain is $A(s)$, while the scaled output (by a factor of b , which may be frequency dependent) is fed back and subtracted from the input. The transfer function is given by

$$H(s) = \frac{V_o(s)}{V_{in}(s)} = \frac{A(s)}{1 - [-A(s)b]} = \frac{A(s)}{1 + T(s)}. \quad (1)$$

The loop gain of the SFG is $T_g(s) = -A(s)b$, and the loop gain of the system, by conventional practice, is $T(s) = -T_g(s)$. If $T(s)$ does not contain right-half plane (RHP) poles, the stability of the system can be determined by the gain and phase margins of $T(s)$ [14].

B. Loop Gains of a Multiloop System

In a system with multiple feedback paths, many loops exist and hence, many loop gains can be defined. Previous research has inferred that not all loop gains are equally practical for stability consideration [4], [6], [12], [15]. The problem is further complicated by the fact that any loop gain can be expressed in many different forms, and even a physically single loop system can be manipulated mathematically to be any of its multiloop equivalents [4]. This ambiguity complicates the interpretation of the loop gain measured, and affects the design of the compensation network to stabilize the system. To overcome the above difficulty, the definition of loop gain in [10] should be adopted. To be more specific, in computing the loop gain of a particular variable, node splitting is performed on that node, e.g., n_k (n_k can be a current, voltage, or any type of variable under investigation), resulting in two nodes, n_{k1} and n_{k2} , with all the incoming branches go to n_{k2} , while all outgoing branches radiate from n_{k1} , as shown in Fig. 2. Let n_{k1} be the input node and n_{k2} be the output node. The loop gain of n_k can then be obtained by the Mason's Gain Formula. The

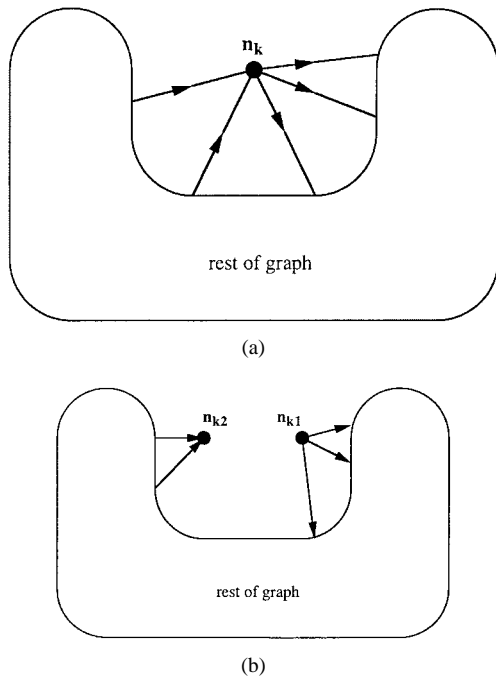


Fig. 2. Node splitting of a SFG.

stability of any linear system is determined by its characteristic polynomial Δ (cited as system determinant in [12]). In SFG analysis, the determinant of the graph relates directly to Δ , and is essential for stability discussion (Section III). It has been demonstrated that Δ can be decomposed in many ways [4] as

$$\Delta = d(s) + n(s) \tag{2}$$

where both $d(s)$ and $n(s)$ are polynomials in s . For design engineers, measuring loop gains is essential in understanding the dynamics of systems. Hence, we need to break (2) up in a way such that the loop gain $T(s)$ [obtained as $T(s) = n(s)/d(s)$] can be measured directly, and the criteria of phase and gain margins can be utilized for stability analysis, provided that $d(s)$ contains no RHP root. Mathematically speaking, the original multiloop system is transformed into an equivalent single loop system with loop gain $T(s)$, so that a familiar method of analysis, e.g., Bode plots, can be applied.

III. SYSTEM LOOP GAIN OF A SWITCHING CONVERTER

In this section, we discuss how the SFG method is applied to analyze switching converters. This result is valid for systems with the same mathematical formulation.

Fig. 4 shows the essential elements of a switching converter. Buck, boost, and buck–boost converters can be obtained through different arrangements of the inductor, power transistor, and the diode (Fig. 3). The output stage consists of a filtering capacitor and a (resistive) load. The output voltage is attenuated by the resistor string R_1 and R_2 , and is fed back to the error amplifier and compared with a reference voltage to determine the trip point of the PWM comparator. The ramp can be a fixed one (voltage programming, Fig. 4) or be scaled by the inductor current (current programming, Fig. 5). In either

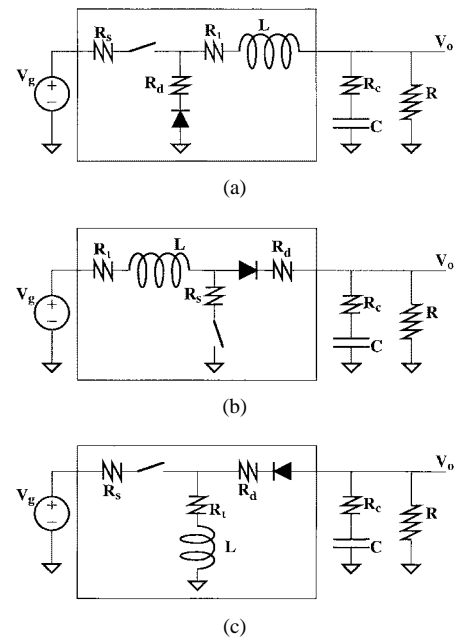


Fig. 3. (a) The buck converter, (b) the boost converter, and (c) the buck–boost converter.

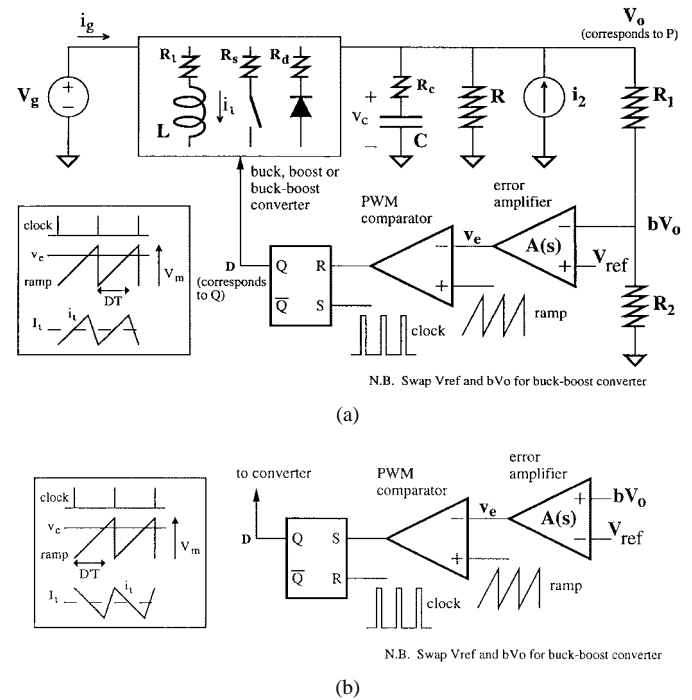


Fig. 4. A generic voltage-programming converter: (a) trailing-edge modulation and (b) leading-edge modulation.

case, from Table I, the perturbed SSA equation is (cf., [1], [3])

$$\dot{\hat{x}} = \mathbf{A}\hat{x} + \mathbf{B}\hat{u} + \mathbf{E}\hat{d} \tag{3}$$

where \hat{x} is the state vector, \hat{u} is the input vector, \hat{d} is the duty ratio, and any matrix $\mathbf{M} = [m_{ij}]$.¹ For second-order converters, the state variables are the capacitor voltage (\hat{v}_c)

¹In this paper, boldface upper case letters are matrices, boldface lower case letters are vectors. In later discussions, \mathbf{I} is the identity matrix, and $\mathbf{0}$, depending on the context, is either the null matrix or the null vector.

TABLE II

ANALYSIS SUMMARY OF THE BUCK CONVERTER (a) STATE-SPACE AVERAGED MATRICES, (b) VOLTAGE PROGRAMMING (FOR BOTH TRAILING- AND LEADING-EDGE MODULATION), (c) CURRENT PROGRAMMING (TRAILING-EDGE MODULATION), AND (d) CURRENT PROGRAMMING (LEADING-EDGE MODULATION)

A	B	E
$\begin{bmatrix} \frac{1}{\alpha CR} & \frac{1}{\alpha C} \\ -\frac{1}{\alpha L} & \frac{1}{L} \end{bmatrix}$	$\begin{bmatrix} 0 & \frac{1}{\alpha C} \\ D & \frac{R_c \parallel R}{L} \end{bmatrix}$	$\begin{bmatrix} 0 \\ \beta \frac{V_g}{L} \end{bmatrix}$
C	D	F
$\begin{bmatrix} \frac{1}{\alpha} & R_c \parallel R \\ \frac{1}{\alpha} & D \end{bmatrix}$	$\begin{bmatrix} 0 & R_c \parallel R \\ 0 & 0 \end{bmatrix}$	$\begin{bmatrix} 0 \\ \frac{\eta D V_g}{R} \end{bmatrix}$

$$\text{Voltage transformation ratio: } \frac{V_o}{V_g} = \eta D$$

(a)

G	H
$\begin{bmatrix} A(s)b & A(s)bR_c \\ \alpha V_m & \alpha V_m \end{bmatrix}$	$\begin{bmatrix} 0 \\ \frac{A(s)bR_c}{\alpha V_m} \end{bmatrix}$

$$T(s) = A(s)b \frac{1}{D} \frac{V_o}{V_m} \frac{1 + \frac{s}{\omega_z}}{1 + \frac{1}{Q} \frac{s}{\omega_o} + \frac{s^2}{\omega_o^2}}$$

(b)

G_a	G_b
$\frac{\gamma}{\alpha n_1 D T} \frac{1}{V_g} \frac{L}{R_f} [1 \ R_c]$	$\begin{bmatrix} \gamma D & 1 \\ \alpha n_1 D' & V_g \end{bmatrix} \frac{\gamma \lambda_1}{n_1 D' T} \frac{L}{V_g}$
H_a	H_b
$\frac{\gamma}{\alpha n_1 D' T} \frac{L}{V_g} \frac{R_c}{R_f} [0 \ 1]$	$\begin{bmatrix} -\gamma D & 1 \\ n_1 D' & V_g \end{bmatrix} \frac{\gamma}{\alpha n_1 D' T} \frac{D R_c}{V_g}$

$$T(s) = A(s)b \frac{R \parallel R_a}{R_f} \frac{1 + s/\omega_z}{1 + \left(\frac{1}{\omega_a} + \frac{R \parallel R_a}{R} \frac{1}{\omega_{t1}} \right) s + \frac{s^2}{\omega_a \omega_{t1}}}$$

$$= A(s)b \frac{R \parallel R_a}{R_f} \frac{1 + \frac{s}{\omega_z}}{\left(1 + \frac{s}{\omega_a} \right) \left(1 + \frac{s}{\omega_{t1}} \right)}$$

(c)

G_a	G_b
$\frac{\gamma}{\alpha n_2 D T} \frac{1}{V_g} \frac{L}{R_f} [1 \ R_c]$	$\begin{bmatrix} \gamma D' & 1 \\ \alpha n_2 D & V_g \end{bmatrix} \frac{\gamma \lambda_2}{n_2 D T} \frac{L}{V_g}$
H_a	H_b
$\frac{\gamma}{\alpha n_2 D T} \frac{L}{V_g} \frac{R_c}{R_f} [0 \ 1]$	$\begin{bmatrix} 0 \\ \frac{\gamma D' R_c}{\alpha n_2 D V_g} \end{bmatrix}$

$$T(s) = A(s)b \frac{R \parallel R_b}{R_f} \frac{1 + s/\omega_z}{1 + \left(\frac{1}{\omega_b} + \frac{R \parallel R_b}{R} \frac{1}{\omega_{t2}} \right) s + \frac{s^2}{\omega_b \omega_{t2}}}$$

$$\approx A(s)b \frac{R \parallel R_b}{R_f} \frac{1 + \frac{s}{\omega_z}}{\left(1 + \frac{s}{\omega_b} \right) \left(1 + \frac{s}{\omega_{t2}} \right)}$$

(d)

Abbreviations

$$b = \frac{R_2}{R_1 + R_2}$$

$$\beta = 1 + \frac{\eta D (R_d - R_s)}{R} \approx 1$$

$$\delta = \frac{R_c / \alpha + R_1 + D R_s + D' R_d}{R} \approx 0$$

$$\lambda_1 = 1 - (R_c \parallel R + R_1 + R_s) \frac{D T}{L} \approx 1$$

$$\lambda_2 = 1 - (R_c \parallel R + R_1 + R_d) \frac{D' T}{L} \approx 1$$

$$\omega_c = \frac{1}{C R}$$

$$\omega_o = \frac{1}{\sqrt{L C}}$$

$$\omega_{t1} = \frac{1}{n_1 D' T}$$

$$\omega_z = \frac{1}{C R_c}$$

$$n_1 = 1 + \frac{m_c}{m_1}$$

$$R_a = \frac{L}{(n_1 D' - D) T}$$

$$R_b = \frac{L}{(n_2 D - D' T)}$$

$$\alpha = 1 + \frac{R_c}{R} \approx 1$$

$$\gamma = 1 + \frac{D (R_s - R_d)}{R + R_1 + R_d} \approx 1$$

$$\eta = \frac{1}{1 + (R_1 + D R_s + D' R_d) / R} \approx 1$$

$$\omega_t = \frac{R}{L}$$

$$Q = \frac{\omega_o}{\omega_c + \delta \omega_1}$$

$$\omega_{t2} = \frac{1}{n_2 D T}$$

$$n_2 = 1 + \frac{m_c}{m_2}$$

$$\omega_a = \frac{1}{C (R \parallel R_a)}$$

$$\omega_b = \frac{1}{C (R \parallel R_b)}$$

and the inductor current (\hat{i}_L). Matrices **A**, **B**, and **E** contain open loop parameters, while \hat{d} is a function of both \hat{x} and \hat{u} , i.e.,

$$\hat{d} = \mathbf{G}\hat{x} + \mathbf{H}\hat{u} \quad (4)$$

which contains feedback quantities such as the gain of the error amplifier $A(s)$ and the attenuation ratio of the resistor string b . In fact, (4) is the control equation of the converter. For loop gain discussion, inputs are irrelevant. Therefore, we set $\hat{u} = \mathbf{0}$, and (3) and (4) combine to read

$$\dot{\hat{x}} = \mathbf{A}\hat{x} + \mathbf{E}\mathbf{G}\hat{x} \quad (5a)$$

$$\begin{bmatrix} \dot{\hat{v}}_c \\ \dot{\hat{i}}_L \end{bmatrix} = \begin{bmatrix} a_{11} & a_{12} \\ a_{21} & a_{22} \end{bmatrix} \begin{bmatrix} \hat{v}_c \\ \hat{i}_L \end{bmatrix} + \begin{bmatrix} e_{11} \\ e_{21} \end{bmatrix} [g_{11} \ g_{12}] \begin{bmatrix} \hat{v}_c \\ \hat{i}_L \end{bmatrix} \quad (5b)$$

and an equivalent SFG can be constructed (Fig. 6). The characteristic polynomial is given by

$$\Delta = \det[s\mathbf{I} - \mathbf{A} - \mathbf{E}\mathbf{G}] \quad (6)$$

while the determinant of the graph is easily computed as

$$\det(\text{graph}) = 1 - \frac{a_{11}}{s} - \frac{a_{22}}{s} - \frac{a_{12}a_{21}}{s^2} - \frac{e_{11}g_{11}}{s} - \frac{e_{21}g_{12}}{s}$$

$$- \frac{a_{12}e_{21}g_{11}}{s^2} - \frac{a_{21}e_{11}g_{12}}{s^2} + \frac{a_{11}}{s} \frac{a_{22}}{s}$$

$$+ \frac{a_{11}}{s} \frac{e_{21}g_{12}}{s} + \frac{a_{22}}{s} \frac{e_{11}g_{11}}{s} \quad (7a)$$

$$= \det[s\mathbf{I} - \mathbf{A} - \mathbf{E}\mathbf{G}] / s^2. \quad (7b)$$

Hence, the determinant of the graph contains complete information on the stability of the converter.

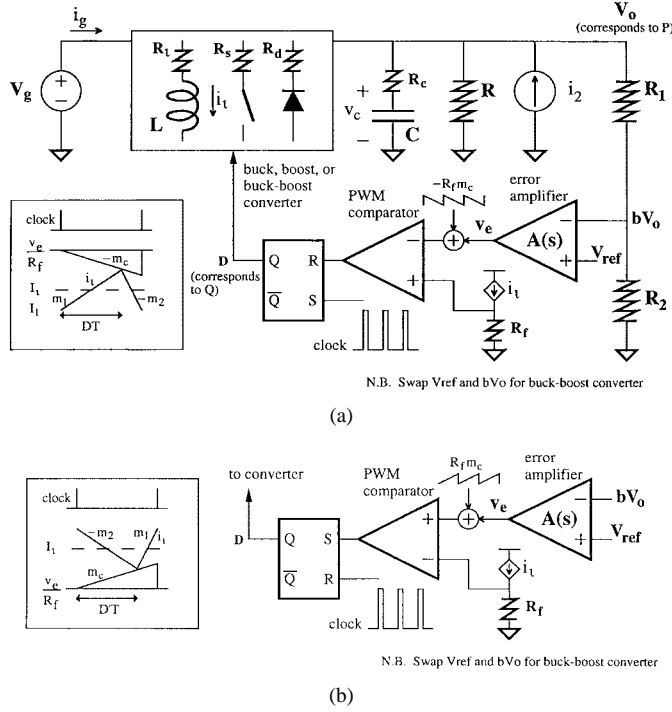


Fig. 5. A generic current-programming converter: (a) trailing-edge modulation and (b) leading-edge modulation.

A. System Loop Gain of a Voltage-Programming Converter

From Fig. 4(a), it is routine to derive the control equation of the converter, i.e., the perturbed duty ratio as a function of the input and state variables

$$\hat{d} = -A(s)b \frac{\hat{v}_o}{V_m} \tag{8}$$

where $\hat{v}_o = \hat{v}_o(\hat{x}, \hat{u})$. Hence, \hat{d} can be expressed as $\hat{d} = \mathbf{G}\hat{x} + \mathbf{H}\hat{u}$, which implies that both g_{11} and g_{12} contain the gain of the error amplifier $A(s)$ and the attenuation factor b , i.e.,

$$\mathbf{G} = [g_{11} \quad g_{12}] = [A(s)bg_{a1} \quad A(s)bg_{a2}] = A(s)b\mathbf{G}_a. \tag{9}$$

The parameters g_{a1} and g_{a2} depend on the converter under consideration, e.g., Table II compiles the parameters for the buck converter.

Now (6) can be partitioned into two parts: the first one contains terms with $A(s)b$, and serves as the numerator $n(s)$ in (2), while the remaining terms are grouped as the denominator $d(s)$. This partitioning is important because $A(s)b$ is related to the feedback path that gives the locations of breaking the loop physically, as shown by the nodes P (related to the output \hat{v}_o) and Q (corresponds to \hat{d}) in Figs. 4 and 7. With the above partitioning, the system loop gain is then given by (10a), shown at the bottom of the page, which can easily be

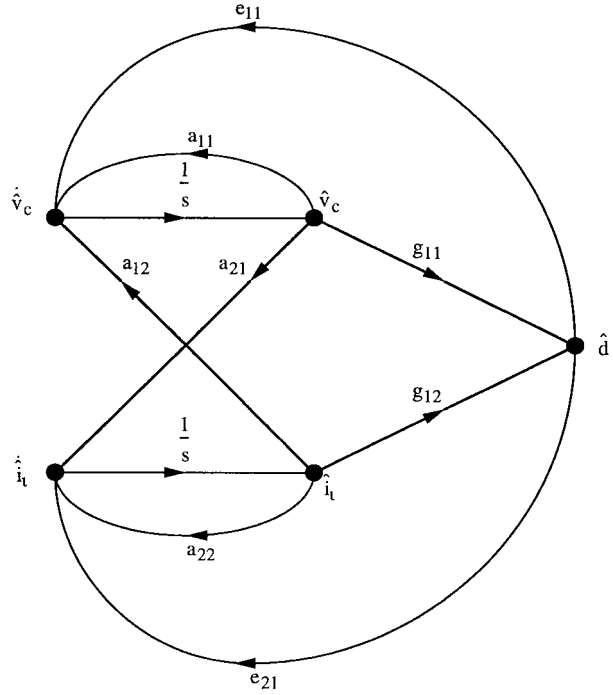


Fig. 6. SFG of a power converter.

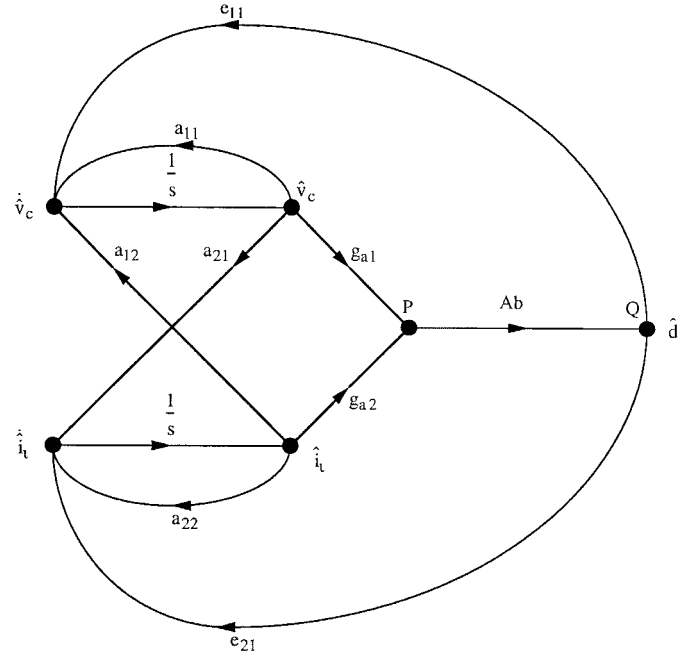


Fig. 7. SFG of a voltage programming converter.

verified as

$$T(s) = -\text{trace}([s\mathbf{I} - \mathbf{A}]^{-1}\mathbf{E}\mathbf{G}) \tag{10b}$$

$$= -A(s)b \text{trace}([s\mathbf{I} - \mathbf{A}]^{-1}\mathbf{E}\mathbf{G}_a) \tag{10c}$$

$$= -\frac{\text{trace}[\text{adj}(s\mathbf{I} - \mathbf{A})\mathbf{E}\mathbf{G}]}{\det(s\mathbf{I} - \mathbf{A})} \tag{10d}$$

$$T(s) = -A(s)b \frac{(s - a_{11})e_{21}g_{a2} + (s - a_{22})e_{11}g_{a1} + a_{12}e_{21}g_{a1} + a_{21}e_{11}g_{a2}}{(s - a_{11})(s - a_{22}) - a_{12}a_{21}} \tag{10a}$$

where for any matrix \mathbf{M} , $\text{trace}(\mathbf{M})$ is the trace of \mathbf{M} , and $\text{adj}(\mathbf{M})$ is the adjoint of \mathbf{M} . A more direct way of computing $T(s)$ makes use of a lesser known result. By construction, \mathbf{E} is an $n \times 1$ matrix, while \mathbf{G} is an $1 \times n$ matrix, therefore, $\text{rank}(\mathbf{E}) = \text{rank}(\mathbf{G}) = \text{rank}(\mathbf{EG}) = 1$, and (6) can then be decomposed² as [16]

$$\det[s\mathbf{I} - \mathbf{A} - \mathbf{EG}] = \det[s\mathbf{I} - \mathbf{A}] \{1 - \text{trace}([s\mathbf{I} - \mathbf{A}]^{-1}\mathbf{EG})\} \quad (11)$$

and (10b) follows immediately [cf. (2)].

The advantage of arriving at (10c) becomes apparent. If $\det[s\mathbf{I} - \mathbf{A}]$ contains no RHP root, then the gain and phase margins can be used to determine the stability of the converter. Moreover, one can modify $A(s)$ with a compensation network by changing $A(s)$ to some $A_{\text{comp}}(s)$, and the above discussion on stability still applies. As for $\det[s\mathbf{I} - \mathbf{A}]$, the roots are the poles of the open loop converter, which reside in the left-half plane (LHP).

As mentioned previously, P and Q are the two locations for breaking the loop. Injection at P (which relates to v_o , bv_o , and v_e) can be done by analog method [11], while injection at Q (corresponds to the output of the latch) has to be done digitally [12]. With a node splitting at either P or Q , and Mason's gain formula used to compute the loop gain, (10a) is obtained. Hence, for voltage-programming converters, the loop gains measured by either analog or digital injection are the same.

From Fig. 6, two observations are made. First, no other node splitting can result in the above $T(s)$. For example, if node splitting is performed at either \hat{v}_c or \hat{i}_L , then the inductor current and capacitor voltage loop gains are given by $T_{xv}(s)$ and $T_{xi}(s)$, respectively, with

$$\mathbf{T}_x(s) = \begin{bmatrix} T_{xv}(s) & Z_x(s) \\ Y_x(s) & T_{xi}(s) \end{bmatrix} = [s\mathbf{I} - \mathbf{A} - \mathbf{EG}]^{-1}\mathbf{EG}. \quad (12)$$

$Z_x(s)$ and $Y_x(s)$ are the closed loop transimpedance and transadmittance, respectively. Note that $T(s)$ cannot be directly obtained from (12). Second, except for nodes P or Q , other nodes are inaccessible for loop breaking. For example, \hat{v}_c is inside the capacitor. The external node of a capacitor already includes its equivalent series resistance (ESR).

B. System Loop Gain of a Current-Programming Converter

For current-programming converters, we refer to Table I and Fig. 5 (also see [17]), and learn that for converters with

²For \mathbf{A} and \mathbf{B} both 2×2 matrices, it can be shown, e.g., by direct expansion, that

$$\begin{aligned} \det(\mathbf{A} + \mathbf{B}) &= \det(\mathbf{A}) + \det(\mathbf{B}) + \text{trace}[\text{adj}(\mathbf{A})\mathbf{B}] \\ &= \det(\mathbf{A}) + \det(\mathbf{B}) + \text{trace}[\text{adj}(\mathbf{B})\mathbf{A}]. \end{aligned}$$

If $\det(\mathbf{B}) = 0$, then

$$\det(\mathbf{A} + \mathbf{B}) = \det(\mathbf{A}) + \text{trace}[\text{adj}(\mathbf{A})\mathbf{B}] = \det(\mathbf{A})[1 + \text{trace}(\mathbf{A}^{-1}\mathbf{B})].$$

Similarly, for \mathbf{A} and \mathbf{B} both 3×3 matrices, we have

$$\det(\mathbf{A} + \mathbf{B}) = \det(\mathbf{A}) + \det(\mathbf{B}) + \text{trace}[\text{adj}(\mathbf{A})\mathbf{B}] + \text{trace}[\text{adj}(\mathbf{B})\mathbf{A}].$$

trailing-edge modulation, the control equation is

$$\hat{d} = -\frac{1}{n_1 m_1 T} \hat{i}_L - \frac{D}{n_1 m_1} \hat{m}_1 + \frac{1}{n_1 m_1 T R_f} \hat{v}_e \quad (13a)$$

where m_1 and m_c are the slopes of the inductor current and the compensation ramp in State 1, respectively. The switching frequency is $f_s = 1/T$, n_1 is the slope factor defined as $n_1 = 1 + m_c/m_1$, \hat{v}_e is the perturbed output of the error amplifier, and R_f is the equivalent current sensing resistor. For converters with leading-edge modulation, the control equation is

$$\hat{d} = -\frac{1}{n_2 m_2 T} \hat{i}_L + \frac{D'}{n_2 m_2} \hat{m}_2 + \frac{1}{n_2 m_2 T R_f} \hat{v}_e \quad (13b)$$

where m_2 is the slope of the inductor current in State 2 and $n_2 = 1 + m_c/m_2$ the corresponding slope factor. From (13a) and (13b), it is clear that the factor $A(s)b$ cannot be factored out, and \mathbf{G} takes the following form:

$$\mathbf{G} = [g_{11} \quad g_{12}] \quad (14a)$$

$$= [A(s)bg_{a1} + g_{b1} \quad A(s)bg_{a2} + g_{b2}]$$

$$= A(s)b\mathbf{G}_a + \mathbf{G}_b \quad (14b)$$

i.e., both g_{11} and g_{12} contain terms that are not multiplied by $A(s)b$. The corresponding SFG is shown in Fig. 8. Decomposing the system determinant as in the previous section, and noting that $\text{rank}(\mathbf{EG}_a) = \text{rank}(\mathbf{EG}_b) = 1$, we get

$$\begin{aligned} \det[s\mathbf{I} - \mathbf{A} - \mathbf{EG}] &= \det[s\mathbf{I} - \mathbf{A} - \mathbf{EG}_b] \\ &\cdot \{1 - A(s)b \text{trace}([s\mathbf{I} - \mathbf{A} - \mathbf{EG}_b]^{-1}\mathbf{EG}_a)\} \end{aligned} \quad (15)$$

and $T(s)$ can be obtained as

$$T(s) = -A(s)b \text{trace}([s\mathbf{I} - \mathbf{A} - \mathbf{EG}_b]^{-1}\mathbf{EG}_a) \quad (16a)$$

which can further be simplified as³

$$= -A(s)b \frac{\text{trace}[\text{adj}(s\mathbf{I} - \mathbf{A})\mathbf{EG}_a]}{\det(s\mathbf{I} - \mathbf{A} - \mathbf{EG}_b)}. \quad (16b)$$

The above system loop gain can be obtained directly by a node splitting at P (analog injection), but not at node Q (digital injection). If node Q is chosen, the loop gain is given by (10b) but not (10c), since in this case, $\mathbf{G} \neq A(s)b\mathbf{G}_a$. On expanding the terms, we get

$$T_Q(s) = -\frac{A(s)bn_1(s) + n_2(s)}{\det(s\mathbf{I} - \mathbf{A})} \quad (\text{node splitting at } Q) \quad (17)$$

where $n_1(s) = \text{trace}[\text{adj}(s\mathbf{I} - \mathbf{A})\mathbf{EG}_a]$ and $n_2(s) = \text{trace}[\text{adj}(s\mathbf{I} - \mathbf{A})\mathbf{EG}_b]$ (cf., [3]). The difference in (16b) and (17) explains the discrepancy in the loop gain measurement observed in [12]. We should also point out that (17) is not suitable for design, because modifying $A(s)$ for compensation requires addition of numerators that cannot be drawn easily on a Bode plot. A more serious problem is that the denominator does not give the correct pole locations of the closed loop system. To conclude, the only suitable point to perform loop gain measurement is at P , as shown in Figs. 5 and 8.

³By direct expansion, $\text{adj}(\mathbf{A} + \mathbf{B}) = \text{adj}(\mathbf{A}) + \text{adj}(\mathbf{B})$. Also, for \mathbf{E} an $n \times 1$ matrix, and \mathbf{G}_a and \mathbf{G}_b any $1 \times n$ matrices, $\text{adj}(\mathbf{EG}_b)\mathbf{EG}_a = \mathbf{0}$.

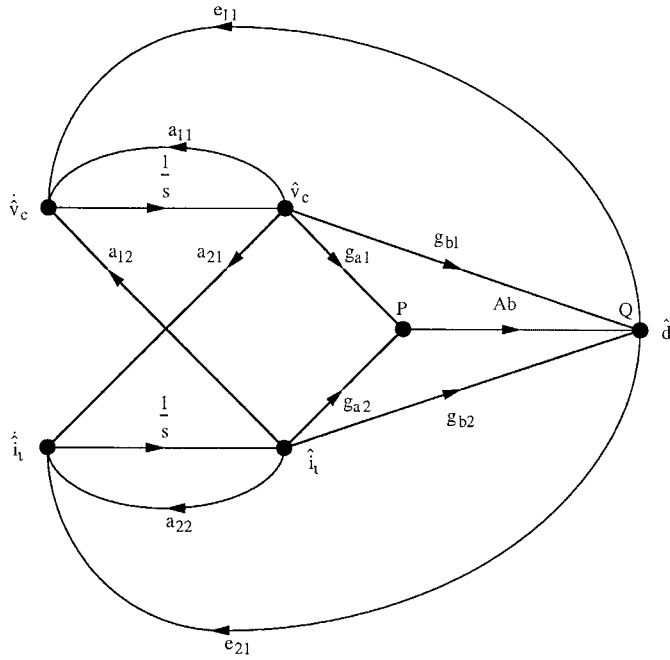


Fig. 8. SFG of a current-programming converter.

IV. APPLICATION OF THE ANALYSIS

We demonstrate the validity of the analysis by applying it to the generic buck–boost converter. The following analyses include certain parasitic elements, such as the ESR of the filtering capacitor R_c , series resistance of the inductor R_i , and resistance of the diode R_d and of the switch R_s . To simplify the expressions, we assign all Greek variables to be related to parasitics, with $\delta \ll 1$, or, in the limit of no parasitic elements, $\delta = 0$, while others, such as α , β , γ , η , and λ are all approximately equal to one. If parasitic elements are absent, $\alpha = \beta = \gamma = \eta = \lambda = 1$.

A. Analysis of the Voltage-Programming Buck–Boost Converter

Fig. 3(c) shows a generic buck–boost converter. Continuous conduction mode is assumed, and two states of operation can be identified. In State 1, $t \in [nT, (n+D)T]$, the switch is closed, and the inductor current i_l ramps up, while in State 2, $t \in [(n+D)T, (n+1)T]$, and i_l ramps down. The state vector $\mathbf{x}(t)$ contains two elements, the capacitor voltage v_c and the inductor current i_l . The generator voltage v_g (with a dc value of V_g) and an output injection current i_2 constitute the input vector $\mathbf{u}(t)$. Note that i_2 is used for computing the

output impedance of the converter and has a steady-state value of $I_2 = 0$ (Figs. 4 and 5). The output vector $\mathbf{y}(t)$ consists of the output voltage v_o and the input current i_g needed for input impedance computation. A routine analysis gives the matrices \mathbf{A}_1 , \mathbf{B}_1 , \mathbf{C}_1 , and \mathbf{D}_1 in State 1, and \mathbf{A}_2 , \mathbf{B}_2 , \mathbf{C}_2 , and \mathbf{D}_2 in State 2. Performing SSA gives the \mathbf{A} , \mathbf{B} , \mathbf{C} , and \mathbf{D} matrices as shown in Table IV. To compute the steady state \mathbf{x}_o and \mathbf{y}_o , we need the determinant of \mathbf{A}

$$\det(\mathbf{A}) = \frac{1}{\alpha\eta} \frac{D'^2}{LC} \quad (18)$$

where all parameters are defined in Table IV. The steady-state capacitor voltage and inductor current are given by

$$\mathbf{x}_o = \begin{bmatrix} V_c \\ I_l \end{bmatrix} = -\mathbf{A}^{-1}\mathbf{B}\mathbf{u}_o = \begin{bmatrix} -\eta \frac{D}{D'} V_g \\ \eta \frac{D}{D'^2} \frac{V_g}{R} \end{bmatrix} \quad (19)$$

and the steady-state output voltage and input current are

$$\mathbf{y}_o = \begin{bmatrix} V_o \\ I_g \end{bmatrix} = [-\mathbf{C}\mathbf{A}^{-1}\mathbf{B} + \mathbf{D}]\mathbf{u}_o = \begin{bmatrix} -\eta \frac{D}{D'} V_g \\ \eta \frac{D^2}{D'^2} \frac{V_g}{R} \end{bmatrix}. \quad (20)$$

Observe that $V_o = V_c$ and $I_g = DI_l$. These results are to be expected, since the output voltage is the sum of the capacitor voltage and the voltage across the ESR. In steady state, no net charge is dumped into the capacitor, and the current going in and out of the filtering capacitor develops positive and negative voltages across the ESR, respectively. Although power is dissipated in the ESR, the average voltage is zero, and $V_o = V_c$. For the second result, observe that during State 1, $i_g = i_l$, while during State 2, $i_g = 0$, and hence the average I_g is only DI_l . Also, the efficiency η of the converter can be obtained from (20) as

$$\eta = \frac{V_o I_o}{V_g I_g} = \frac{D'^2(R + R_c)}{D'^2 R + D' R_c + \alpha(R_i + D R_s + D' R_d)}. \quad (21)$$

Next, performing perturbation analysis as shown in Table I gives the \mathbf{E} and \mathbf{F} matrices. For the voltage-programming buck–boost converter, the control equation is $\hat{d} = A(s)b\hat{v}_o/V_m$. With minor computation, the \mathbf{G} and \mathbf{H} matrices are obtained [Table IV(b)]. Clearly, the matrix \mathbf{G}

$$T(s) = -\frac{A(s)b}{\alpha D'} \frac{V_g}{V_m} \text{trace} \left(\begin{bmatrix} s + \frac{1}{\alpha C R} & \frac{D'}{\alpha C} \\ -\frac{D'}{\alpha L} & s + \frac{R_\delta}{L} \end{bmatrix}^{-1} \begin{bmatrix} \frac{\eta}{\alpha} \frac{D}{D'} \frac{1}{C R} & -\frac{\eta}{\alpha} \frac{D}{D'} \frac{R_c}{C R} \\ \frac{1}{L} & -\frac{R_c}{L} \end{bmatrix} \right) \quad (23a)$$

$$\approx \frac{A(s)b}{D D'} \frac{|V_o|}{V_m} \frac{1 + \frac{s}{\omega_d}}{1 + \frac{1}{Q} \frac{s}{\omega_o} + \frac{s^2}{\omega_o^2}} \quad (23b)$$

is of the form $A(s)b\mathbf{G}_a$ [cf., (9)] and the system loop gain is given by (10d), which is

$$T(s) = -\text{trace}([s\mathbf{I} - \mathbf{A}]^{-1}\mathbf{E}\mathbf{G}) \quad (22a)$$

$$= -\frac{A(s)b}{\alpha D'} \frac{V_g}{V_m} \cdot \text{trace} \left(\begin{bmatrix} 2 + \frac{1}{\alpha CR} & \frac{D'}{\alpha C} \\ -\frac{D'}{\alpha L} & s + \frac{R_\delta}{L} \end{bmatrix}^{-1} \begin{bmatrix} \frac{\eta}{\alpha} \frac{D}{D'} \frac{1}{CR} & 0 \\ \frac{1}{L} & 0 \end{bmatrix} \right) \quad (22b)$$

$$\approx \frac{A(s)b}{DD'} \frac{|V_o|}{V_m} \frac{1 - \frac{s}{\omega_z}}{1 + \frac{1}{Q} \frac{s}{\omega_o} + \frac{s^2}{\omega_o^2}}. \quad (22c)$$

All variables are defined in Table IV, with $R_\delta = \delta R$. It is clear from (22c) that the system loop gain contains a RHP zero that moves with the load. This zero could be at a very low frequency. Dominant pole compensation will result in a converter with very limited bandwidth.

For the buck–boost converter with leading-edge modulation, the corresponding \mathbf{G} and \mathbf{H} matrices are shown in Table IV(c), and the system loop gain is given in (23a) and (23b) at the bottom of the previous page. The dc gain and the poles are the same as in the case with trailing-edge modulation, yet the zero is different. Clearly, in order to put ω_d in the LHP, we need

$$CR_c \geq \frac{D}{D'} \frac{R}{L}. \quad (24)$$

In applying the same analysis method to the boost converter [Fig. 3(b)], it can be shown that the corresponding condition to give a LHP zero is $CR_c \geq D'R/L$, which is the same as that derived in [8], confirming the validity of the system loop gain. The following physical interpretation is in place. For a current-programming converter, the inductor current is used to define the trip point. For the boost (and buck–boost) converter, the inductor current passes through the filtering capacitor in State 2, but not in State 1. Hence, for trailing-edge modulation, whence the trip point is evaluated at the end of State 1, the ESR does not show up in the zero ω_z . But for leading-edge modulation, the trip point is evaluated at the end of State 2, and the presence of the ESR tends to move the RHP zero to the left. If C or R_c is large enough, a LHP zero will be obtained in (23a) and (23b).

B. Analysis of the Current-Programming Boost Converter

In this section, analysis of current-programming boost converters are considered [Fig. 3(b)] so that results can be compared to those derived in [4]. A straightforward application of the procedure described in Table I gives matrices \mathbf{A} – \mathbf{H} (Table III). We now focus on the computation of the system loop gain. For simplicity's sake, assume that all components are ideal.

From previous discussion, \mathbf{G} is of the form $A(s)b\mathbf{G}_a + \mathbf{G}_b$, and (16c) should be used to compute the system loop gain.

Simple computation gives

$$\text{trace}[\text{adj}(s\mathbf{I} - \mathbf{A})\mathbf{E}\mathbf{G}_a] = -\frac{1}{n_1 D'T} \frac{D'}{CR_f} \left(1 - \frac{sL}{D'^2 R} \right) \quad (25a)$$

$$\det[s\mathbf{I} - \mathbf{A} - \mathbf{E}\mathbf{G}_b] = s^2 + \left(\frac{1}{CR} + \frac{1}{n_1 D'T} \right) s + \frac{1}{n_1 D'T} \frac{1}{C} \left(\frac{1}{R} + \frac{1}{R} + \frac{n_1 D'^3 T}{L} \right) \quad (25b)$$

and gives the system loop gain as

$$T(s) = A(s)bD' \frac{R||R||R_a}{R_f} \frac{1 - s/\omega_z}{1 + \left[\frac{1}{\omega_a} + \frac{(R||R||R_a)/R}{\omega_{t1}} \right] s + \frac{s^2}{\omega_a \omega_{t1}}} \quad (26a)$$

with all parameters defined in Table III. In general, $\omega_{t1} \gg \omega_a$, hence,

$$T(s) \approx A(s)bD' \frac{R||R||R_a}{R_f} \frac{1 - s/\omega_z}{\left(1 + \frac{s}{\omega_a} \right) \left(1 + \frac{s}{\omega_{t1}} \right)}. \quad (26b)$$

For current-programming converter with leading-edge modulation, the system loop gain is given by

$$T(s) \approx A(s)bD' \frac{R||R||R_b}{R_f} \frac{1 + s/\omega_d}{\left(1 + \frac{s}{\omega_b} \right) \left(1 + \frac{s}{\omega_{t2}} \right)}. \quad (27)$$

Again, see Table III for definitions of parameters. Note that leading-edge modulation could move the RHP zero to the LHP if appropriate condition is met.

V. VERIFICATION OF ANALYSIS

The validity of the mentioned analysis will be demonstrated by comparing results with published works that have been confirmed by experiments. Several examples are presented to illustrate the robustness of this new method.

A. Boost Converter with Voltage-Programming

The control mechanism of trailing-edge modulation is different from that of leading-edge modulation, and [8] is the first paper to investigate this difference on a boost converter. By applying the so-called “discrete average model,” the control-to-output transfer function for the trailing-edge modulated converter is

$$\frac{\hat{v}_o}{\hat{d}} = \frac{V_g}{D'^2} \frac{1 - s/\omega_z}{1 + s/\omega_o Q + s^2/\omega_o^2} \quad (\text{trailing-edge}) \quad (28)$$

where all parameters are defined in Table III. From Section III-A, we have $\hat{d} = -A(s)b\hat{v}_o/V_m$. Now, consider the breaking of the loop at the output of the converter. With the \hat{v}_o from

TABLE III
ANALYSIS SUMMARY OF THE BOOST CONVERTER (a) STATE-SPACE AVERAGED MATRICES, (b) VOLTAGE PROGRAMMING (TRAILING-EDGE MODULATION), (c) VOLTAGE PROGRAMMING (LEADING-EDGE MODULATION), (d) CURRENT PROGRAMMING (TRAILING-EDGE MODULATION), AND (e) CURRENT PROGRAMMING (LEADING-EDGE MODULATION)

A	B	E	G	H
$\begin{bmatrix} 1 & D' \\ \alpha CR & \alpha C \\ D & \delta R \\ \alpha L & L \end{bmatrix}$	$\begin{bmatrix} 0 & 1 \\ 1 & D' R_c \\ L & \alpha L \end{bmatrix}$	$\begin{bmatrix} \eta & V_g \\ \alpha D^2 CR & \beta \eta V_g \\ \alpha D' L & \alpha D' L \end{bmatrix}$	$\begin{bmatrix} A(s)b & \\ \alpha V_m & 0 \end{bmatrix}$	$\begin{bmatrix} 0 & A(s)bR_c \\ & \alpha V_m \end{bmatrix}$
$\begin{bmatrix} 1 & D' R_c \\ \alpha & \alpha \\ 0 & 1 \end{bmatrix}$	$\begin{bmatrix} 0 & R_c \parallel R \\ 0 & 0 \end{bmatrix}$	$\begin{bmatrix} -\eta R_c & V_g \\ \alpha R & D'^2 \\ 0 & 0 \end{bmatrix}$	$T(s) = A(s)b \frac{1}{1-D} \frac{V_o}{V_m} \frac{1 - \frac{s}{\omega_z}}{1 + \frac{1}{Q} \frac{s}{\omega_o} + \frac{s^2}{\omega_o^2}}$	

$$\text{Voltage transformation ratio: } \frac{V_o}{V_g} = \eta \frac{1}{1-D}$$

(a)

(b)

G	H	G _a	G _b	H _a	H _b
$\begin{bmatrix} A(s)b & A(s)bR_c \\ \alpha V_m & \alpha V_m \end{bmatrix}$	$\begin{bmatrix} 0 & A(s)bR_c \\ & \alpha V_m \end{bmatrix}$	$\begin{bmatrix} -\gamma_1 & D' & L & 1 \\ \alpha n_1 D' T & V_g & R_f & 0 \end{bmatrix}$	$\begin{bmatrix} 0 & -\gamma_1 \lambda_1 & D' & L \\ n_1 D' T & V_g & & \end{bmatrix}$	$\begin{bmatrix} 0 & -\gamma_1 & D' & L & R_c \\ \alpha n_1 D' T & V_g & R_f & & \end{bmatrix}$	$\begin{bmatrix} -\gamma_1 & DD' & 1 \\ n_1 D' T & V_g & 0 \end{bmatrix}$
$T(s) = A(s)b \frac{1}{1-D} \frac{V_o}{V_m} \frac{1 + \frac{s}{\omega_d}}{1 + \frac{1}{Q} \frac{s}{\omega_o} + \frac{s^2}{\omega_o^2}}$		$T(s) = A(s)b D' \frac{R \parallel R \parallel R_a}{R_f} \frac{1 - \frac{s}{\omega_z}}{\left(1 + \frac{s}{\omega_a}\right) \left(1 + \frac{s}{\omega_{t1}}\right)}$			

(c)

(d)

$\begin{bmatrix} \gamma_2 & D' & L & 1 \\ \alpha n_2 DT & V_g & R_f & 1 \parallel R_c \end{bmatrix}$	$\begin{bmatrix} \gamma_2 & D'^2 & 1 & -\gamma_2 \lambda_2 & D' & L \\ \alpha n_2 DT & V_g & & n_2 DT & V_g & \end{bmatrix}$
$\begin{bmatrix} 0 & -\gamma_2 & D' & L & R_c \\ \alpha n_2 DT & V_g & R_f & & \end{bmatrix}$	$\begin{bmatrix} -\gamma_2 & D'^2 & 1 & \gamma_2 & D'^2 & R_c \\ n_2 DT & V_g & \alpha n_2 DT & V_g & & \end{bmatrix}$
$T(s) = A(s)b D' \frac{R \parallel R \parallel R_b}{R_f} \frac{1 + \frac{s}{\omega_d}}{\left(1 + \frac{s}{\omega_b}\right) \left(1 + \frac{s}{\omega_{t2}}\right)}$	

Abbreviations

$$\alpha = 1 + \frac{R_c}{R} \quad \beta = 1 + \frac{\alpha R_c \parallel R + R_d - R_s}{R}$$

$$\delta = \frac{R_t + DR_s + D'(R_c \parallel R + R_d)}{R} \approx 0 \quad \eta = \frac{D'^2 (R + R_c)}{D'^2 R + D' R_c + \alpha(R_t + DR_s + D' R_d)} \approx 1$$

$$\omega_o = \frac{D'}{\sqrt{LC}} \quad Q = \frac{\omega_o}{\omega_c + \delta \omega_t}$$

$$\omega_z = \frac{D'^2 R}{L} \quad \omega_d = \frac{1}{\frac{CR_c}{D'} - \frac{L}{D'^2 R}}$$

$$n_1 = 1 + \frac{m_c}{m_1} \quad n_2 = 1 + \frac{m_c}{m_2}$$

$$\omega_1 = \frac{1}{n_1 D' T} \quad \omega_2 = \frac{1}{n_2 DT}$$

$$\gamma_1 = 1 + \frac{\alpha}{D'} \frac{R_t + R_s}{D' R + R_c + \alpha(R_d - R_s)} \approx 1 \quad \gamma_2 = 1 + \frac{D' R_c + \alpha(R_t + R_s)}{D'^2 R + \alpha D' (R_d - R_s)} \approx 1$$

$$\lambda_1 = 1 - (R_t + R_s) \frac{DT}{L} = 1 \quad \lambda_2 = 1 - \left(\frac{R_c + R_t + R_d}{\alpha} \right) \frac{D' T}{L} \approx 1$$

$$R_a = \frac{1}{n_1 D'^3 T} \quad \omega_a = \frac{1}{C(R \parallel R \parallel R_a)}$$

$$R_b = \frac{1}{(n_2 D - 1) D'^2 T} \quad \omega_b = \frac{1}{C(R \parallel R \parallel R_b)}$$

(e)

the expression of \hat{d} as the input, and the \hat{v}_o of (28) as the output, we get

$$T(s) = A(s)b \frac{1}{1-D} \frac{V_o}{V_m} \frac{1 - s/\omega_z}{1 + s/\omega_o Q + s^2/\omega_o^2} \quad (\text{trailing-edge}) \quad (29)$$

which is identical to the system loop gain $T(s)$ given in Table III. To eliminate the RHP zero, [8] applied a heuristic reasoning on the ESR voltage [8, Eqs. (1)–(5)], and arrived at

$$\frac{\hat{v}_o}{\hat{d}} = \frac{V_g}{D'^2} \frac{1 + s/\omega_d}{1 + s/\omega_o Q + s^2/\omega_o^2} \quad (\text{leading-edge}) \quad (30)$$

TABLE IV
ANALYSIS SUMMARY OF THE BUCK-BOOST CONVERTER (a) STATE-SPACE AVERAGED MATRICES, (b) VOLTAGE PROGRAMMING (TRAILING-EDGE MODULATION), (c) VOLTAGE PROGRAMMING (LEADING-EDGE MODULATION), (d) CURRENT PROGRAMMING (TRAILING-EDGE MODULATION), AND (e) CURRENT PROGRAMMING (LEADING-EDGE MODULATION)

A $\begin{bmatrix} 1 & D' \\ \alpha CR & \alpha C \\ D' & R_\delta \\ \alpha L & L \end{bmatrix}$	B $\begin{bmatrix} 0 & 1 \\ D & D'R_c \end{bmatrix}$	E $\begin{bmatrix} \eta D V_g \\ \alpha D^2 CR \\ 1 V_g \\ D' L \end{bmatrix}$	G $\begin{bmatrix} A(s)b \\ \alpha V_m & 0 \end{bmatrix}$	H $\begin{bmatrix} 0 & A(s)bR_c \\ \alpha V_m \end{bmatrix}$
C $\begin{bmatrix} 1 & D'R_c \\ \alpha & D' \end{bmatrix}$	D $\begin{bmatrix} 0 & R_c \parallel R \\ 0 & 0 \end{bmatrix}$	F $\begin{bmatrix} \eta D \\ \alpha D^2 V_g \\ \eta D \\ \alpha D^2 R \end{bmatrix}$	$T(s) = A(s)b \frac{1}{DD'} \frac{ V_o }{V_m} \frac{1 - \frac{s}{\omega_z}}{1 + \frac{1}{Q} \frac{s}{\omega_o} + \frac{s^2}{\omega_o^2}}$	

$$\text{Voltage transformation ratio: } \frac{V_o}{V_g} = -\eta \frac{D}{1-D}$$

(a)

(b)

G $\begin{bmatrix} A(s)b & -A(s)bR_c \\ \alpha V_m & \alpha V_m \end{bmatrix}$	H $\begin{bmatrix} 0 & A(s)bR_c \\ \alpha V_m \end{bmatrix}$	G_a $\begin{bmatrix} \gamma_1 D' L & 1 \\ \alpha n_1 D' T V_g R_f & 0 \end{bmatrix}$	G_b $\begin{bmatrix} 0 & -\gamma_1 \lambda_1 D' L \\ n_1 D' T V_g & 0 \end{bmatrix}$
C $\begin{bmatrix} 1 & D'R_c \\ \alpha & D' \end{bmatrix}$	D $\begin{bmatrix} 0 & R_c \parallel R \\ 0 & 0 \end{bmatrix}$	H_a $\begin{bmatrix} \gamma_1 D' L & 1 \\ \alpha n_1 D' T V_g R_f & 0 \end{bmatrix}$	H_b $\begin{bmatrix} -\gamma_1 D' L & 1 \\ n_1 D' T V_g & 0 \end{bmatrix}$

$$T(s) = A(s)b \frac{1}{DD'} \frac{|V_o|}{V_m} \frac{1 + \frac{s}{\omega_d}}{1 + \frac{1}{Q} \frac{s}{\omega_o} + \frac{s^2}{\omega_o^2}}$$

(c)

(d)

G_a $\begin{bmatrix} \gamma_2 D' L & 1 \\ \alpha n_2 DT V_g R_f & [1 \quad -R_c] \end{bmatrix}$	G_b $\begin{bmatrix} -\gamma_2 D^2 L & -\gamma_2 \lambda_2 D' L \\ \alpha n_2 D V_g & n_2 DT V_g \end{bmatrix}$
H_a $\begin{bmatrix} \gamma_2 D' L & 1 \\ \alpha n_2 DT V_g R_f \end{bmatrix}$	H_b $\begin{bmatrix} -\gamma_2 D^2 R_c \\ \alpha n_2 D V_g \end{bmatrix}$

$$T(s) = A(s)b \frac{1-D}{1+D} \frac{R \parallel R_b}{R_f} \frac{1 + \frac{s}{\omega_d}}{\left(1 + \frac{s}{(1+D)\omega_b}\right) \left(1 + \frac{s}{\omega_{t2}}\right)}$$

Abbreviations

$$\alpha = 1 + \frac{R_c}{R} \approx 1 \quad \beta = 1 + \frac{\alpha R_c \parallel R + R_d - R_s}{D R} \approx 1$$

$$\delta = \frac{R_1 + DR_\delta + D'(R_c \parallel R + R_d)}{R} \approx 0 \quad R_\delta = \delta R$$

$$\eta = \frac{(1-D)^2 (R + R_c)}{(1-D)^2 R + (1-D)R_c + \alpha(R_1 + DR_s + D'R_d)} \approx 1$$

$$\omega_c = \frac{1}{CR} \quad \omega_1 = \frac{R}{L}$$

$$\omega_o = \frac{1-D}{\sqrt{LC}} \quad Q = \frac{\omega_o}{\omega_c + \delta\omega_1}$$

$$\omega_z = \frac{D^2 R}{D' L} \quad \omega_d = \frac{1}{\frac{CR_c}{D'} - \frac{D' L}{D^2 R}}$$

$$n_1 = 1 + \frac{m_c}{m_1} \quad n_2 = 1 + \frac{m_c}{m_2}$$

$$\omega_{t1} = \frac{1}{n_1 D' T} \quad \omega_{t2} = \frac{1}{n_2 DT}$$

$$\gamma_1 = 1 + \frac{D}{D' D' R / \alpha + R_c / \alpha + R_1 + R_d} \approx 1 \quad \gamma_2 = \frac{1}{\eta [1 + (R_1 + R_d) / (D' R)]} \approx 1$$

$$\lambda_1 = 1 - (R_1 + R_s) \frac{DT}{L} \approx 1 \quad \lambda_2 = 1 - \left(\frac{R_c}{\alpha} + R_1 + R_d \right) \frac{D' T}{L} \approx 1$$

$$R_a = \frac{1+D}{n_1 D'^3 T} \quad \omega_a = \frac{1}{C(R \parallel R_a)}$$

$$R_b = \frac{1+D}{(n_2 D - 1) D'^2 T} \quad \omega_b = \frac{1}{C(R \parallel R_b)}$$

(e)

which gives the same $T(s)$ as shown in Table III. We should emphasize that our proposed method assumes no *ad hoc* reasoning. The difference of the system loop gains is accounted for by the difference in the control equations.

B. Boost Converter with Current-Programming

For current-programming converters, it should be noted that [4, eq. (13)] is inaccurate, as has been discussed in [17]. With

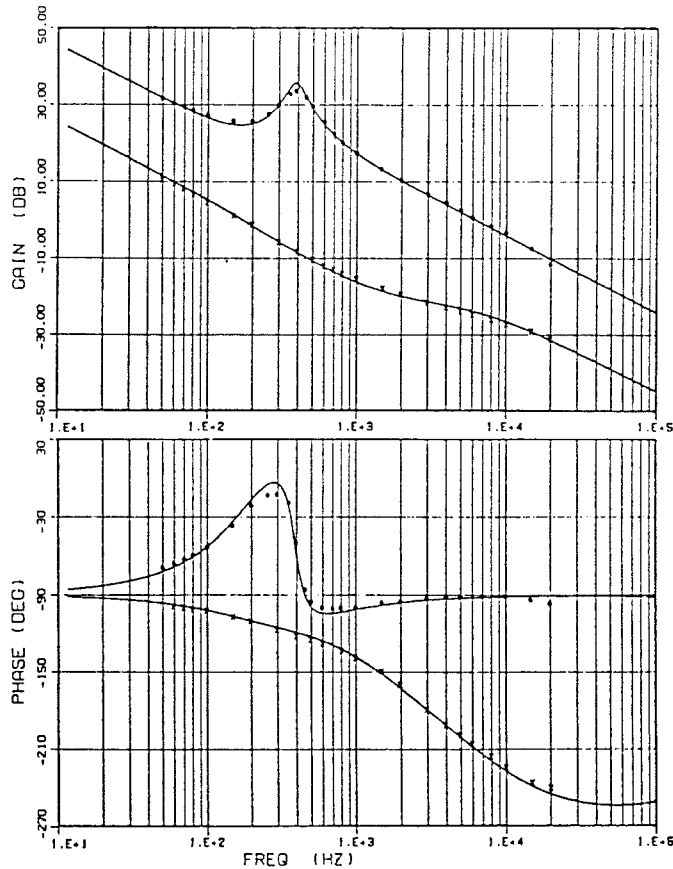


Fig. 9. The Bode plots of the loop gains T1 and T2 for the CIC system: — — — theoretical predictions of T1 and T2, ···· T1 measured at the point A, * * * * T2 measured at the point C using the analog modulator.

the correct control equation of (13a), and using the y_{2c} and y_{22} in [4, Table 1], [4, eq. (50)] reads

$$\frac{\hat{v}_o}{\hat{v}_e} = D' \frac{R||R||R_a}{R_f} \frac{1 - s/\omega_z}{\left(1 + \frac{s}{\omega_a}\right)\left(1 + \frac{s}{\omega_{t1}}\right)} \quad (31)$$

which gives the same $T(s)$ as discussed in Section IV (26b).

C. Analog Versus Digital Loop Gain Measurement

In [12], a loop gain measurement method using a digital modulator was introduced. The method was applied to measure the loop gain of the boost converter (with trailing-edge modulation). For the voltage-programming converter, both the digital and analog methods yield agreeable results ([12, Fig. 16]). For the current-programming converter (termed as charge injection control, or CIC in [12]), the Bode plot of the loop gain by the analog method ([12, curve T1, Fig. 15], which is reproduced as Fig. 9 in this paper) showed clearly the existence of a low-frequency pole, a RHP zero, and a high-frequency pole, which copes well with (31), while the digital method gave a loop gain with a local peaking at 400 Hz (curve T2, Fig. 9), a typical curve for a pair of complex poles. This loop gain is predicted by (17), but our discussion suggested that it is not useful for stability consideration.

VI. CONCLUSION

A unified method in analyzing dc-dc CCM switch mode power converters is presented. The advantages of this approach lie in its uniformity in deriving system loop gains of converters, and its power in explaining discrepancies exist in the literature. The first assertion is demonstrated in Sections III and IV, where buck, boost, or buck-boost converters with either voltage- or current-programming employing either trailing- or leading-edge modulation are analyzed with the same method. The only difference is the control equations for different converters. The second assertion is demonstrated by explaining the difference in measuring loop gains using analog and digital injections. We also want to emphasize the following points.

- 1) The characteristic polynomial, rather than arbitrarily defined loop gains, should be used to determine the stability of the converter.
- 2) By grouping terms in the characteristic polynomial that contains $A(s)b$ as the numerator and the rest as the denominator, a unique system loop gain can be defined. The criteria of gain and phase margins can thus be applied to determine the stability of the converter, and based on which an appropriate compensation network can be designed.
- 3) By method of SFG, appropriate locations (P and Q in Figs. 4, 5, 7, and 8) are identified for breaking the loop.
- 4) For voltage-programming converters, both analog and digital loop gain measurements give the same result.
- 5) For current-programming converters, analog loop gain measurement gives the system loop gain, while digital loop gain measurement gives a transfer function with the numerator corrupted by terms that do not contain $A(s)b$, and the gain and phase margin thus obtained is not directly usable for designing the compensation network.

ACKNOWLEDGMENT

The author would like to thank Prof. W. A. Coles, University of California at San Diego, for his teaching in signal flow graph, Prof. R. D. Middlebrook of the California Institute of Technology for his teachings in design-oriented analysis and Prof. G. C. Temes of Oregon State University, Corvallis, for his inspiration in perturbation analysis, all of which were essential to the completion of this paper.

REFERENCES

- [1] R. Middlebrook and S. Cuk, "A general unified approach to modeling switching-converter power stages," in *Proc. IEEE Power Elec. Specialists Conf.*, 1976, pp. 18-34.
- [2] S. Hsu, A. Brown, L. Rensink, and R. Middlebrook, "Modeling and analysis of switching DC-to-DC converters in constant-frequency current-programmed mode," in *Proc. IEEE Power Elec. Specialists Conf.*, 1979, pp. 284-301.
- [3] D. Mitchell, *DC-DC Switching Regulator Analysis*. New York: McGraw-Hill, 1988.
- [4] R. Middlebrook, "Topics in multiple-loop regulators and current mode programming," in *Proc. IEEE Power Elec. Specialists Conf.*, 1985, pp. 716-732.
- [5] F. Tan and R. Middlebrook, "A unified model for current-programmed converters," *IEEE Trans. Power Electron.*, vol. 10, pp. 397-408, July 1995.

- [6] G. Schoneman and D. Mitchell, "Closed-loop performance comparisons of switching regulators with current-injected control," *IEEE Trans. Power Electron.*, vol. 3, pp. 31–43, Jan. 1988.
- [7] M. Kazimierczuk and R. Cravens, II, "Input impedance of closed-loop PWM buck–boost DC–DC converter for CCM," in *Proc. Int. Symp. Circuits Syst.*, 1995, pp. 2047–2050.
- [8] D. Sable, B. Cho, and R. Ridley, "Elimination of the positive zero in fixed frequency boost and flyback converters," in *IEEE Applied Power Electron. Conf.*, 1990, pp. 205–211.
- [9] K. Smedley and S. Cuk, "Switching flow-graph nonlinear modeling technique," *IEEE Trans. Power Electron.*, vol. 9, pp. 405–413, July 1994.
- [10] S. Mason, "Feedback theory—Some properties of signal flow graphs," *Proc. IRE*, vol. 41, pp. 1144–1156, 1953.
- [11] R. Middlebrook, "Measurement of loop gain in feedback systems," *Int. J. Electron.*, vol. 38, no. 4, pp. 485–512, 1975.
- [12] B. Cho and F. Lee, "Measurement of loop gain with the digital modulator," in *IEEE Power Electron. Specialists Conf.*, 1984, pp. 363–373.
- [13] M. Gopal, *Modern Control System Theory*. New York: Halsted, 1984.
- [14] M. Van Valkenberg, *Network Analysis*. Englewood Cliffs, NJ: Prentice-Hall, 1974.
- [15] R. Ridley, B. Cho, and F. Lee, "Analysis and interpretation of loop gains of multiloop-controlled switching regulators," *IEEE Trans. Power Electron.*, vol. 3, pp. 489–498, Oct. 1988.
- [16] K. Miller, *Some Eclectic Matrix Theory*. Malabar, FL: Krieger, 1987.
- [17] W. Ki, "Analysis of subharmonic oscillation of fixed frequency current-programming switch mode power converters," *IEEE Trans. Circuits Syst. I.*, vol. 45, pp. 104–108, Jan. 1998.



Wing-Hung Ki (S'86–M'91) received the B.Sc. degree in 1984 from the University of California, San Diego, the M.Sc. degree in 1985 from the California Institute of Technology, Pasadena, and the Engineer Degree and the Ph.D. degree from the University of California, Los Angeles, in 1990 and 1995, respectively, all in electrical engineering.

From 1985 to 1986, he was a Research Assistant in the Power Electronic Group of Caltech, Pasadena, CA, helping to develop the software SCAMP (Switching Converter Analysis & Measurement Program). He joined Micro Linear Corporation, San Jose, CA, in 1992 as a Senior Design Engineer in the Department of Power and Battery Management, working on the design of power converter controllers until joining the Hong Kong University of Science and Technology, Clear Water Bay, in 1995 as an Assistant Professor. His research interests include analysis and modeling of switch mode power converters and dimmable electronic ballasts, and fundamental research in analog integrated circuits.